Encounters with the golden ratio in fluid dynamics

M. Mokry
WTISOFT, Ottawa, Canada

Abstract

This paper suggests that the golden ratio, prominent in nature and art, has also its presence in fluid dynamics. The first example draws from the investigation of the resonance in wind tunnels with ventilated walls. Using acoustic wave theory, the reciprocal golden ratio is shown to determine the critical Mach number below which refraction is possible and above which total reflection takes place. The second example concerns the vortex merger, such as observed in aircraft turbulence and large-scale atmospheric or oceanic flows. Based on a numerical simulation and available experimental data, a conjecture is made that the distance below which two identical Rankine vortices merge and above which they do not is the product of the vortex diameter and golden ratio.

Keywords: golden ratio, wind tunnel resonance, vortex merger.

1 Introduction

The ratio

$$\Phi = \frac{a}{b}, \qquad a > b > 0$$

is termed "golden" if

$$\frac{a}{b} = \frac{a+b}{a},$$

implying that the ratio between the greater part, a, and the smaller part, b, is equal to the ratio between the whole, $a+b$, and the greater part, a. Combining the above equations yields

$$\Phi = 1 + \Phi^{-1}, \tag{1}$$

WIT Transactions on Ecology and the Environment, Vol 114, © 2008 WIT Press
www.witpress.com, ISSN 1743-3541 (on-line)
doi:10.2495/DN080131

which has the positive root

$$\Phi = (\sqrt{5}+1)/2 = 1.618\ldots \tag{2}$$

The golden ratio (or section) relates to the Fibonacci sequence in terms of the limit

$$\Phi = \lim_{n\to\infty} \frac{F_{n+1}}{F_n}, \qquad F_{n+1} = F_n + F_{n-1} \quad \text{with } F_0 = 0 \text{ and } F_1 = 1 \tag{3}$$

and has the continued fraction expansion

$$\Phi = [1;1,1,1,\ldots] = 1 + \cfrac{1}{1 + \cfrac{1}{1 + \cfrac{1}{\ddots}}} \quad . \tag{4}$$

In view of these and other appealing algebraic properties [1], the golden ratio can be found in biology, architecture, pictorial arts, music, fig. 1. Claimed to provide the 'divine' proportions, it reflects the sense of a harmonious or pleasing ideal. In fluid dynamics the presence of Φ is less conspicuous, typically disguised in defining the boundaries between different flow patterns.

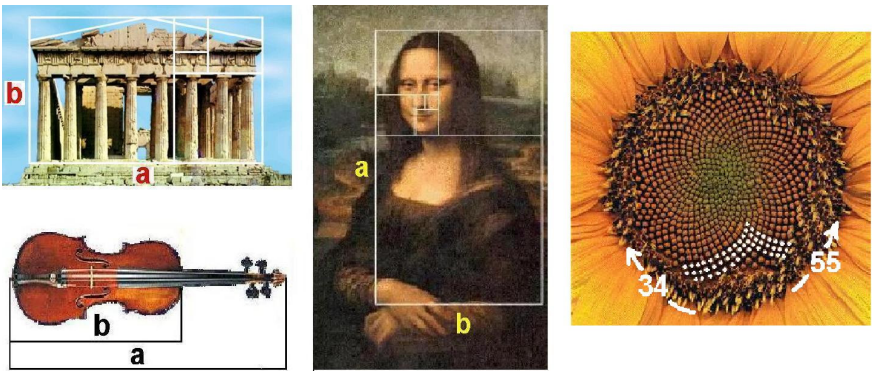

Figure 1: Golden ratio and Fibonacci numbers in art and life.

The first example discussed in this paper is based on the study of the resonance frequencies in ventilated-wall wind tunnels by Mabey [2]. Using experimental observations and acoustic ray theory, he found that the form of the solution changes across a 'special' Mach number, $M = (\sqrt{5}-1)/2 \approx 0.618$. This unexpected subsonic flow divide is more readily accepted once we realize it is Φ^{-1}, cf. eqns. (1) and (2).

Reasoning that the golden ratio plays a more general role in resonance phenomena and the dynamics of nonlinear systems, Schewe [3] independently searched for its presence in the vortices shed by a cylinder in the highly sensitive Reynolds number range of $3–4\times10^5$. From his experimental results it appears that the ratio of Strouhal numbers (based on the vortex shedding frequency)

belonging to the consecutive stable states of the Kármán vortex street was nearly constant, equal to Φ. The author is again obliged to D.G. Mabey [4] for drawing his attention to this resource; unfortunately is not able to offer any new insight based on his own work.

The second part of the paper deals with the symmetric vortex merger, the prototype problem for the merger of like-signed vorticity, such as observed in aircraft turbulence, ocean eddies, and hurricanes. The determination of the critical distance below which two identical Rankine vortices merge and above which they do not is considered analytically intractable. However, based on the available experimental data, a conjecture is made that the ratio of the critical distance and the diameter of the vortices is equal to Φ.

2 Wind tunnel resonance

Wind tunnels resonance has been observed [5] at frequencies of the oscillating model such that the disturbances emanating from the oscillating model reflect from the walls to form a standing wave pattern. If the pressure node is at the model position, the amplitude of the normal force is eliminated or substantially reduced. It has also been found that the resonance frequencies in wind tunnels with open-jet boundaries or ventilated walls (slotted or perforated) differ from those in wind tunnels with solid walls [2,6].

To exemplify the physics involved, consider the propagation of acoustic waves at an infinite interface between the moving air (test section) and still air (plenum chamber), fig.2. Inside the test section, the disturbance velocity potential φ satisfies

$$\left(1-\frac{U^2}{c^2}\right)\frac{\partial^2\varphi}{\partial x^2}+\frac{\partial^2\varphi}{\partial y^2}-2\frac{U}{c^2}\frac{\partial^2\varphi}{\partial x\,\partial t}-\frac{1}{c^2}\frac{\partial^2\varphi}{\partial t^2}=0, \quad \text{test section,} \tag{5}$$

where U is the tunnel stream velocity and c the velocity of sound. In the plenum, φ satisfies

$$\frac{\partial^2\varphi}{\partial x^2}+\frac{\partial^2\varphi}{\partial y^2}-\frac{1}{\tilde{c}^2}\frac{\partial^2\varphi}{\partial t^2}=0, \quad \text{plenum,} \tag{6}$$

where the velocity of sound $\tilde{c}$ is generally different from that in the test section.

For the incident and reflected plane waves, eqn. (5) has the solutions [7,8]

$$\varphi_I=\exp\{ik[(x-Ut)\sin\theta-y\cos\theta+ct]\} \tag{7}$$

and

$$\varphi_R=R\exp\{ik[(x-Ut)\sin\theta+y\cos\theta+ct]\}, \tag{8}$$

where k is the wave number, θ is the angle of incidence and R is the (relative) reflection coefficient. The transmitted potential, derived from eqn.(6) , is

$$\varphi_T=T\exp\left\{i\tilde{k}[x\tilde{a}-y\tilde{b}+\tilde{c}t]\right\}, \tag{9}$$

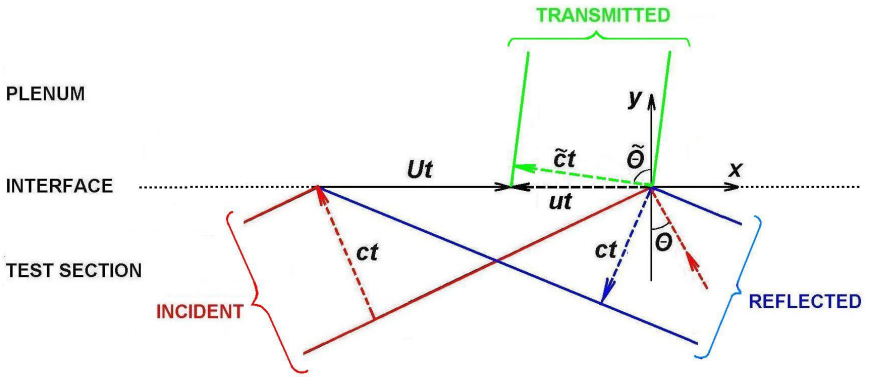

Figure 2: Reflection and refraction of waves at a plane interface.

where $\tilde{k}$ is the wave number in the plenum and T is the (relative) transmission coefficient. The exponential factors $\tilde{a}$ and $\tilde{b}$ in eqn.(9), similarly to $\sin\theta$ and $\cos\theta$ in eqns. (7) and (8), satisfy

$$\tilde{a}^2 + \tilde{b}^2 = 1. \tag{10}$$

From Rayleigh's conditions

$$\frac{c}{\sin\theta} - U = \frac{\tilde{c}}{\tilde{a}} \tag{11}$$

$$k\sin\theta = \tilde{k}\tilde{a}\,. \tag{12}$$

of equal phase velocities and equal wave number components along the interface $y = 0$, we verify that the plane wave solutions (7)-(9) have the common angular frequency

$$\omega = k(c - U\sin\theta) = \tilde{k}\tilde{c} \tag{13}$$

and that

$$\tilde{a} = \tilde{c}\,\frac{\sin\theta}{c - U\sin\theta}\,. \tag{14}$$

The standing wave pattern is possible if the angle of incidence satisfies

$$\sin\theta = \frac{U}{c} = M \tag{15}$$

where $0 < M < 1$ is the stream Mach number. Substituting eqn.(15) in (14) and assuming $\tilde{c} = c$, we obtain

$$\tilde{a} = \frac{M}{1 - M^2}\,. \tag{16}$$

The condition $\tilde{a} < 1$ is synonymous with

$$M < (\sqrt{5} - 1)/2 = \Phi^{-1} \tag{17}$$

In this case

$$\tilde{a} = \sin\tilde{\theta} \qquad \text{and} \qquad \tilde{b} = \sqrt{1-\tilde{a}^2} = \cos\tilde{\theta}\ , \tag{18}$$

where $\tilde{\theta}$ denotes the angle of refraction. Accordingly, eqn.(9) describes a plane wave transmitted into the plenum and eqn.(11) expresses Snell's law. If $M > \Phi^{-1}$, the angle of refraction is imaginary and total reflection takes place. This, however, does not imply that the interface acts like a solid wall: because of phase changes, the situation is more complex than that.

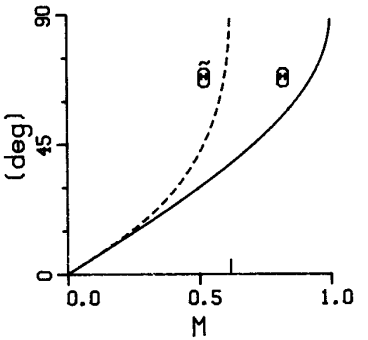

Figure 3: Angles of incidence and refraction at resonance [10].

For the solid interface (closed wall)

$$R = 1 \qquad \text{and} \qquad T = 0 \tag{19}$$

on the entire range of subsonic Mach numbers. For the open-jet interface, as derived by Miles [7],

$$R = \frac{\sin 2\theta - 2\tilde{a}\tilde{b}}{\sin 2\theta + 2\tilde{a}\tilde{b}} \qquad \text{and} \qquad T = \frac{4\tilde{a}\cos\theta}{\sin 2\theta + 2\tilde{a}\tilde{b}} \tag{20}$$

Using eqns. (10) and (15)–(16), the modulus and phase of the reflection coefficient are evaluated and plotted in fig.4 as functions of the Mach number. The abscissa $M = \Phi^{-1}$ is in both graphs indicated by the vertical dotted line. The modulus $|R|$ vanishes at $M = 0$ and $M = M_B = \sin\theta_B \approx 0.564$, where θ_B is Brewster's angle. Putting $|R| = 0$ and $\theta = \theta_B$ it follows from eqns. (18) and (20) that $\theta_B + \tilde{\theta}_B = \pi/2$, confirming that the reflected and transmitted waves are perpendicular to each other, in analogy to electromagnetic waves [9]. On the interval $0 < M < M_B$ the reflection coefficient is negative ($\arg R = \pi$) and small ($\max|R| \approx 0.075$), indicating that resonance is insignificant. On the interval $M_B < M < \Phi^{-1}$ the reflection coefficient is positive ($\arg R = 0$) and of a rapidly increasing magnitude, $|R| \to 1$ as

$M \to \Phi^{-1}$. Interestingly, resonance of the 'closed-wall type' at $M = \Phi^{-1}$ is common to all types of ventilated walls [2]. As shown in fig.4, in the upper subsonic interval $\Phi^{-1} < M < 1$ the modulus is at its maximum, $|R| = 1$, while $\arg R$ grows monotonically from 0 to π.

From eqns. (13) in (15)

$$\frac{\omega}{U} = \frac{1 - M^2}{M} k$$

and, assuming the pressure node at the model position, the (reduced) resonance frequencies are found to be [10]

$$\frac{\omega_n}{U} = \frac{1 - M^2}{M} k_n = [(2n-1)\pi + \arg R] \frac{\sqrt{1 - M^2}}{M h}, \; n = 1, 2, \ldots \quad (21)$$

where n is the resonance mode and h is the distance of the walls between which the standing wave pattern occurs. For the solid walls, in accordance with eqn. (19), $\arg R = 0$. For open-jet boundaries, $\arg R$ varies as indicated in fig. 4b. If $|R| = 1$, resonance is pure, else it is partial.

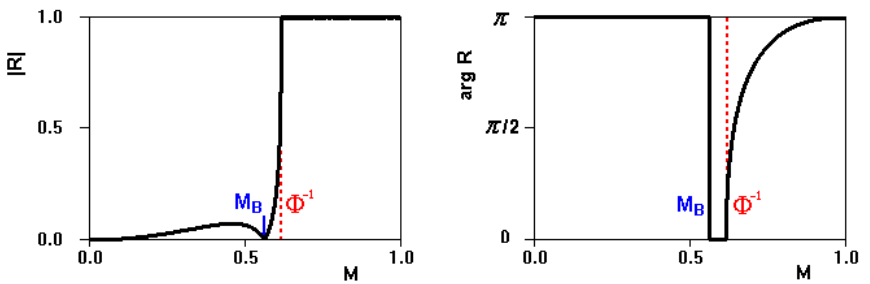

a) modulus b) phase

Figure 4: Reflection coefficient for an open-jet interface.

3 Vortex merger

An important fluid-dynamics phenomenon where the golden ratio is suspected to play a role is the merger of two equal-size vortices of the same orientation. It is the prototype of the vortex merger observed in aircraft turbulence and large-scale atmospheric or oceanic flows. Hurricanes (or cyclones) sometimes pair in such way, fig.5, and are known to orbit about the mutual centre of vorticity (Fujiwhara effect). However, unlike the ocean eddies, they seldom merge. This, presumably (and fortunately), is due to their relatively short lives and large separation distances with respect to their sizes.

There has been a great deal of research devoted to vortex merger in two-dimensional flow, with particular emphasis on the case of two identical vortices

(symmetric merger). The interaction of two identical Rankine vortices (which have cores of uniform vorticity), simulated by the advection of thin, concentric vortex sheets [11] is shown in fig.6. However, the determination of the critical separation distance, below which the merger takes place and above which it does not, has proven difficult computationally and intractable analytically [12]. From the numerical simulation in fig.6 it appears that the merger does not come about until the vortex patches, subjected to mutual strain, become sufficiently distorted to initialize a localized roll-up.

Figure 5: Cyclones Ione (left) and Kirsten (right), 1974. (NOAA Photo Library).

Since from the initial conditions it is not readily apparent whether merger will take place or not, the key to solving this problem is the limit as the number of vortex orbits tends to infinity. Unfortunately, this may not be an easy path to follow because, due to the conservation laws, the efficiency [13] of the merger decreases near the critical distance. This is illustrated in the left-hand picture sequence of fig. 6, where the combined vortex is surrounded by a sea of filamentary debris.

According to the veritable experimental results by Griffiths and Hopfinger [14], the critical distance scaled by the radius of the vortex core is $D^*/r = 3.3 \pm 0.2$. Putting $D^* = 2R^*$, where R^* is the critical orbit radius, $R^*/r = \Phi$ immediately becomes the prime candidate. In support of this conjecture we recall the Pythagorean construction of the golden ratio. In the context of two circular vortices, fig.7, we confirm that the geometrical determination of R^* is as simple as can be expected for this fundamental

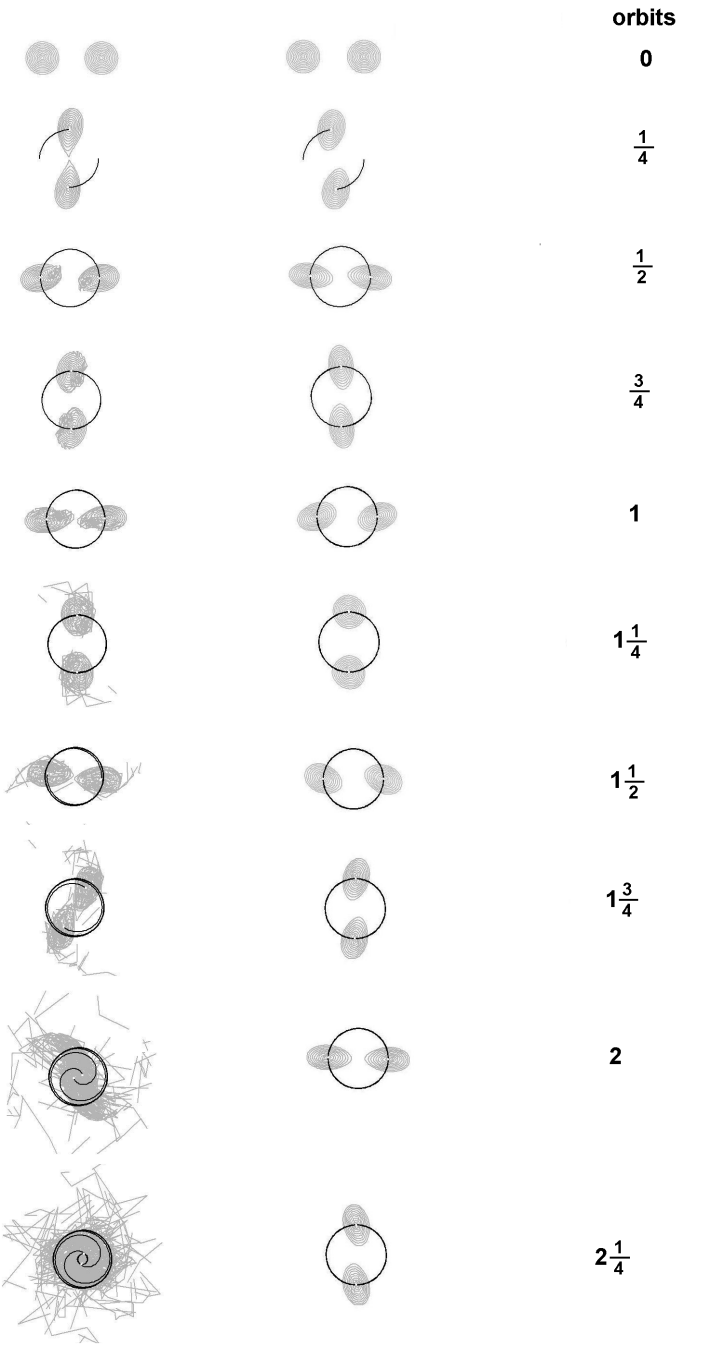

a) merger b) non-merger

Figure 6: Interaction of circular vortex patches simulated numerically [11].

configuration (requiring a straight edge and a pair of compasses only). From the algebraic point of view, Φ is known to have the slowest-converging continued fraction representation, eqn.(4), of all irrational numbers [15]. There may be a connection between an infinitely slow convergence and the infinite number of vortex orbits at the critical distance. However, proving it is a different matter.

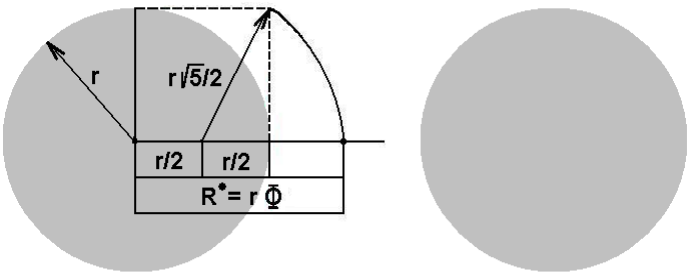

Figure 7: Geometrical construction of the critical orbit radius for two identical Rankine vortices.

4 Discussion

From the preceding analyses it appears that the golden ratio in fluid dynamics does not have the same impact as in biology (Fibonacci-sequence growth) or in architecture and pictorial arts (ideal proportions). On can argue that the introduction of Φ in fluid dynamics is pretentious because, unlike π or e, this irrational number is easily bypassed by its constituent $\sqrt{5}\ (=2\Phi-1)$. We have therefore narrowed our focus to cases where it appears without additive constants: Φ^{-1} in Mabey's tunnel resonance case and Φ both in Schewe's vortex shedding (not analyzed in detail) and the symmetric vortex merger. In all instances the identification of the golden ratio is based on experimental observations. The tunnel resonance result is further supported by acoustic wave theory. For the symmetric vortex merger it is merely a conjecture that, in any case, seems to provide a reasonable estimate of the critical distance normalized by the vortex diameter.

References

[1] Ghyka, M., *The Geometry of Art and Life*, Dover, New York, 1977.
[2] Mabey, D.G., Resonance frequencies in ventilated wind tunnels, *AIAA Journal*, **18(1),** pp. 7–8, 1980.
[3] Schewe, G., Experimental observation of the 'golden section' in flow round a circular cylinder, *Physics Letters*, **109A(1-2),** pp. 47–50, 1985.
[4] Mabey, D.G., Private communication, 9 January 1986, Royal Aircraft Establishment, UK.

[5] Runyan, H.L., Woolston, D.S., and Rainey, A.G., Theoretical and experimental investigation of the effect of tunnel walls on the forces on an oscillating airfoil in two-dimensional subsonic compressible flow. NACA Rep.1262, 1955.
[6] Lee, I., Plenum chamber effect on wind-tunnel resonance by the finite-element method, *AIAA Journal*, **26 (9)**, pp. 1087–1093, 1988.
[7] Miles, J.W., On the reflection of sound at an interface of relative motion, *Journal of the Acoustical Society of America***, 29(2)**, pp. 226–228, 1957.
[8] Barger, R.L., Reflection and transmission of sound by a slotted wall separating two moving fluid streams, NACA TN 4295, 1958.
[9] Born, M. and Wolf, E., *Principles of Optics*, 4th ed., Pergamon Press, Oxford, 1970, pp. 41–51.
[10] Mokry, M., Prediction of resonance frequencies for ventilated wall wind tunnels, *Wind Tunnels and Testing Techniques*, AGARD-CP-348, Paper No.15, Cesme, Turkey, 1983.
[11] Mokry, M., The vortex merger factor in aircraft wake turbulence, *The Aeronautical Journal* , **109(1091)**, pp.13–22, 2005.
[12] Amoretti, M., Durkin, D., Fajans, J., Pozzoli, R., and Rome, M., Asymmetric vortex merger: experiments and simulations, *Physics of Plasmas*, **8(9)**, pp.3865-3868, 2001.
[13] Waugh, D.W., The efficiency of symmetric vortex merger, *Physics of Fluids A* , **4(8)**, pp.1745-1758, 1992.
[14] Griffiths, R.W. and Hopfinger, E.J., Coalescing of geostropic vortices, *Journal of Fluid Mechanics* , **178(73)**, pp.73-97, 1987.
[15] Schroeder, M.R., *Number Theory in Science & Communication*, Springer, New York, 1984, p.58.